



SAPIENZA  
UNIVERSITÀ DI ROMA

Environmental engineering for climate change and mitigation  
Remote Sensing and Geo Big Data

Prof. Mattia Crespi & Prof. Roberta Ravanelli

## **Exercise Report**

By : Hengameh Salari

# MANAGING REFERENCE FRAMES, DATUMS AND COORDINATE SYSTEMS ■

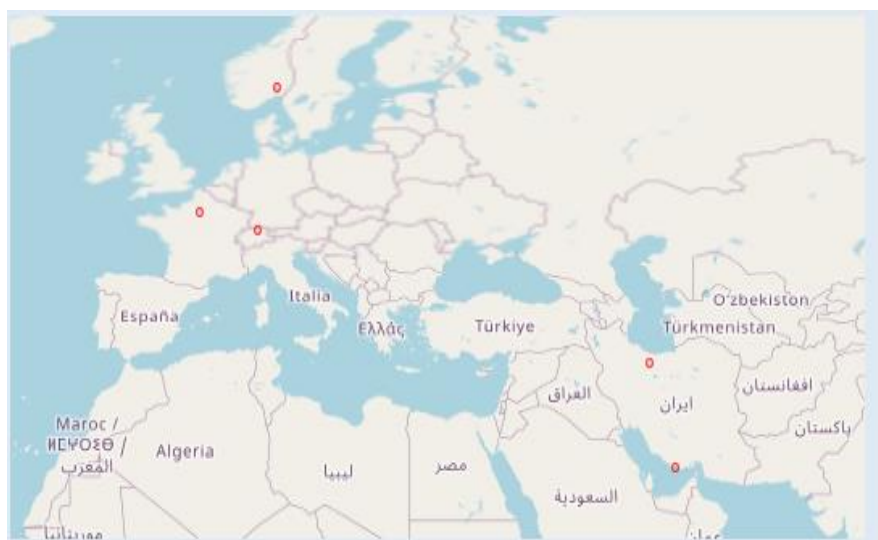
EXERCISE 1 - Reference frame transformations and coordinate system conversions

## Introduction:

As the world continues to advance technologically, there is a growing need for accurate information about various areas on the globe. This information is required for civil purposes, security considerations, and general monitoring. However, due to the dynamic nature of the Earth, it is crucial to utilize both online and offline reference frames and tools such as Global Navigation Satellite Systems (GNSS) and Geographic Information Systems (GIS). One challenge that arises in this context is the accuracy error associated with these tools. To address this, dedicated GNSS systems can be employed, which offer a high level of precision ranging from 1 millimeter to 1 centimeter. In our efforts to achieve our objectives, we make use of the WGS84 coordinate system and perform several coordinate transformations. These measures help us in attaining the desired level of accuracy and efficiency.

1. For this exercise, we begin by selecting 5 points 3 in Europe and 2 in other places. These points are chosen within Google Earth, and the reference frame we use is WGS84, which is a realization of the International Terrestrial Reference System (ITRS). Initially, the accuracy provided by Google is 6 decimal degrees for latitude and longitude, which corresponds to a precision of decimeters. However, for elevation, the accuracy provided by Google is 1 meter. Therefore, the accuracy of latitude and longitude measurements is 0.1 meter, while the accuracy of orthometric height measurements is 1 meter. To facilitate data organization, we have prepared an XLS table where the latitude, longitude, and orthometric heights of the selected points can be entered.

point	LATITUDE-WGS84(ITRF2014) (DEGREES)	LONGITUDE-WGS84(ITRF2014) (DEGREES)	ORTHO HEIGHT (METERS)
1	59,912,401	10,734,120	9
2	47,372,262	8,541,283	414
3	48,861,193	2,336,046	35
4	35,744,801	51,221,664	1272
5	26,546,381	54,021,021	8
Accuracy	(0.1 M)	(0.1 M)	(1 M)



2.The Orthometric Heights of the points obtained from Google Earth can be transformed into Ellipsoidal Heights by utilizing the EGM2008 geoid model, which can be accessed at <http://icgem.gfz-potsdam.de/calcpoints>. By visiting this website, we can locate the Geoid Height information in the final section of the site's results. The Ellipsoidal Height can then be calculated using the formula  $h = H + N$ , where N represents the Geoid undulation, H denotes the orthometric height, and h represents the geodetic height. The accuracy of the Geoid undulation is 0.15 meter, while the accuracy of the ellipsoidal height is 1 meter.

ORTHO HEIGHT (METERS)	GEOIDAL UND. (EGM2008) (METERS)	ELL. HEIGHT - WGS84(ITRF2014) (METERS)
9	39.08	48
414	50.83	465
35	44.74	80
1272	3.9	1276
8 (1 M)	-59.97	-52

**Table 2. Geoidal UND and Ellipsoidal height**

3.In this stage of the exercise, our objective is to convert the WGS84 latitude, longitude, and ellipsoidal height ( $\phi$ ,  $\lambda$ , h) coordinates (known as ellipsoidal coordinates) into WGS84 geocentric cartesian coordinates (X, Y, Z). To achieve this transformation, we make use of the National Geodetic Survey's tool available at <https://geodesy.noaa.gov/NCAT/>. This online resource provides the necessary calculations for the coordinate conversion. It is important to note that the accuracy of this transformation is specified as 1 meter.

Convert/Transform from:

- Horizontal  Horizontal+height  XYZ

Select the type of horizontal coordinate:

- Geodetic lat-long  SPC  UTM  USNG

Select a height

- Ellipsoidal  Orthometric



*Enter lat-lon in decimal degrees*

Lat

Lon

*or degrees-minutes-seconds*

Lat

Lon

*or drag map marker to a location of interest*

Ellipsoid Height

Units of height

Input reference frame (historically called 'horizontal datum')

Output referenc (historically call datum')

*Don't see a reference frame in the list? Click here to learn more.*

Ellipsoid

Reference Frame:

Lat-Lon-Height		SPC		UTM/USNG		XYZ (m)	
Latitude	N35° 44' 41.28360" N354441.28360 35.7448010000	Zone	N/A	Zone	<input type="text" value="39"/>	X	3,246,550.741
Longitude	E51° 13' 17.99040" E0511317.99040 51.2216640000	Northing	N/A (m) N/A (usft) N/A (ift)	Northing (m)	3,955,666.405	Y	4,041,022.687
Ellipsoid Height (m)	1272.000	Easting	N/A (m) N/A (usft) N/A (ift)	Easting (m)	520,042.233	Z	3,705,989.614
		Convergence (dms)	N/A	Convergence (dms)	00 07 46.17		
		Scale factor	N/A	Scale factor	0.99960495		
		Combined factor	N/A	Combined factor	0.99940542		
				USNG	39SWV2004255666		

X-WGS84(ITRF2014) (METERS)	Y- WGS84(ITRF2014) (METERS)	Z-WGS84(ITRF2014) (METERS)
3,149,485,923.00	597,044,263.00	5,495,632,437.00
4,279,611.73	642,745.04	4,670,196.08
4,200,601.95	171,360.62	4,780,443.75
3,246,550.74	4,041,022.69	3,705,989.61
3,354,284.78	4,620,341.07	2,833,346.44
(1 M)	(1 M)	(1 M)

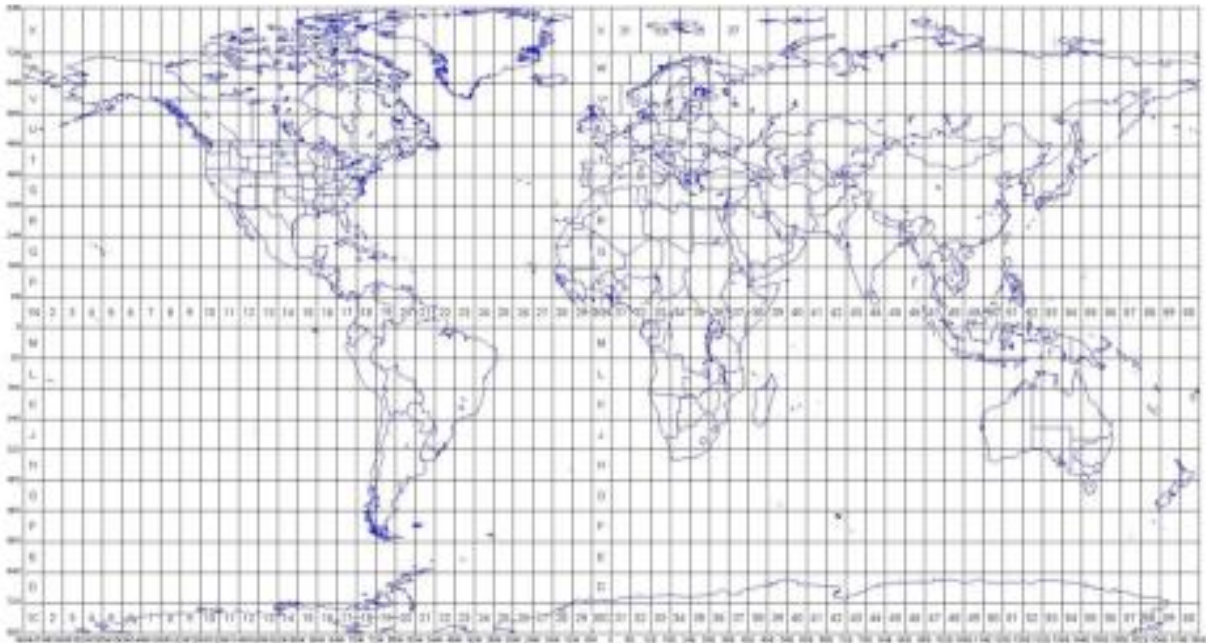
TABLE 3-WGS84 (X, Y, Z)

4. To convert WGS84 latitude and longitude into UTM-WGS84 North and East cartographic coordinates with an accuracy of 0.1 meter, we can use the NOAA's National Geodetic Survey (NGS) website's tool called "NCAT" (National Geodetic Survey Coordinate Conversion and Transformation).

Reference Frame:

Lat-Lon-Height		SPC		UTM/USNG		XYZ (m)	
Latitude	N35° 44' 41.28360" N354441.28360 35.7448010000	Zone	N/A	Zone	<input type="text" value="39"/>	X	3,246,550.741
Longitude	E51° 13' 17.99040" E0511317.99040 51.2216640000	Northing	N/A (m) N/A (usft)	Northing (m)	3,955,666.405	Y	4,041,022.687
		Easting	N/A (m) N/A (usft)	Easting (m)	520,042.233	Z	3,705,989.614
Ellipsoid Height (m)	1272.000	Convergence	N/A (dms) N/A (ift)	Convergence (dms)	00 07 46.17		
		Scale factor	N/A	Scale factor	0.99960495		
		Combined factor	N/A	Combined factor	0.99940542		
				USNG	39SWV2004255666		

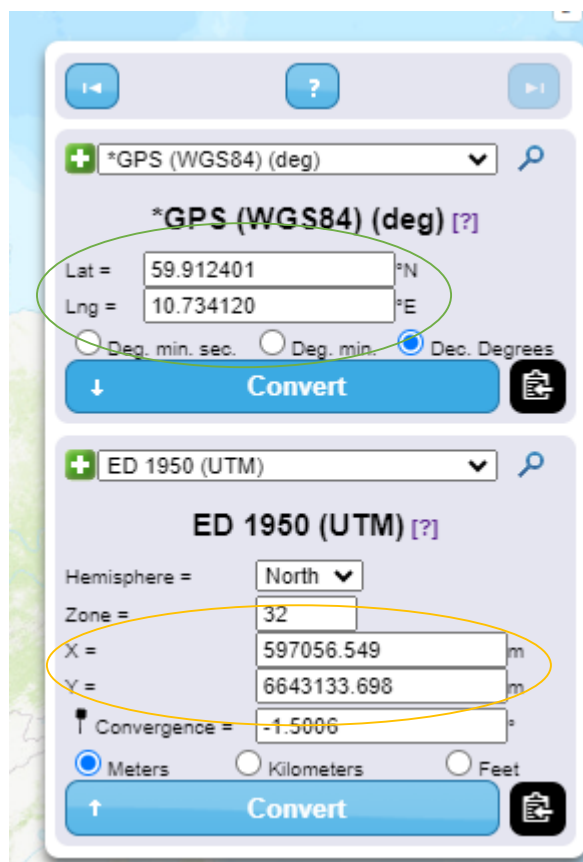
You may change the default UTM zone. The change is processed interactively once a lat-long is converted; DO NOT click the Submit button.



UTM-ZONE-STR	E-UTM-WGS84(ITRF2014) (METERS)	N-UTM-WGS84(ITRF2014) (METERS)
32-V	596,973.43	6,642,925.47
32-T	465,368.77	5,246,635.59
31-U	451,302.07	5,412,237.96
39-S	520,042.23	3,955,666.41
40-R	203,182.69	2,939,644.97
	(0.1 M)	(0.1 M)

TABLE 4-UTM-WGS84 NORTH AND EAST

5.To convert UTM-WGS84 coordinates to UTM-ED50 (European Datum 1950) coordinates using the International Ellipsoid, we should use the TWCC (Two Way Coordinate Conversion) website.





	E-UTM-ED1950	N-UTM-ED1950
	(METERS)	(METERS)
Point 1	597,056.55	6,643,133.70
Point 2	465,451.14	5,246,835.09
Point 3	451,394.10	5,412,445.62

Delta E	Delta N
-83.12	-208.22
-82.37	-199.50
-92.03	-207.66
4.09	-169.74
20.71	-161.37

**6.** in this step for points in Europe we may suppose that our original WGS84 coordinates are ITRF2014 coordinates referred to the epoch of the image indicated within Google Earth; transform WGS84 (X,Y,Z) geocentric cartesian coordinates into ETRF2000 (X,Y,Z) geocentric cartesian coordinates,

It is important to highlight in this report that numerous European countries still depend on their individual national data. Nevertheless, an expanding number of these data are now connected to the European Terrestrial Reference Frame (ETRF). To delve deeper into this matter, we conducted computations for a specific location in Europe. By taking into account velocity components of 0.01 (Vx), 0.02 (Vy), and 0.03 (Vz) meters per year, we determined the ETRF2000 Cartesian coordinate system.

```

Station_1 3149485923 597044263 5495632437 0.01 0.2 0.03
station_2 4279611.728 642745.036 4670196.075 0.01 0.2 0.03
station_3 4200601.947 171360.621 4780443.747 0.01 0.2 0.03
station_4 3246550.741 4041022.687 3705989.614 0.01 0.2 0.03
station_5 3354284.783 4620341.065 2833346.442 0.01 0.2 0.03

```

## RESULTS

#_Station	Frame	Epoch	X[m]	Y[m]	Z[m]	VX[m/yr]	VY[m/yr]	VZ[m/yr]
Station_1	ETRF2000	2023.25	3149486460.0620	597043777.0148	5495632208.3054	15.7044	-13.9855	-6.6148
station_2	ETRF2000	2023.25	4279612.2639	642744.4661	4670195.6528	0.0241	0.1819	0.0187
station_3	ETRF2000	2023.25	4200602.4296	171360.0583	4780443.3253	0.0226	0.1821	0.0187
station_4	ETRF2000	2023.25	3246551.6417	4041022.2781	3705989.3181	0.0348	0.1866	0.0224
station_5	ETRF2000	2023.25	3354285.6893	4620340.6558	2833346.1420	0.0349	0.1866	0.0223

X-ETRF2000 (METERS)	Y-ETRF2000 (METERS)	Z-ETRF2000 (METERS)
3,149,486,460.06	597,043,777.01	5,495,632,208.31
4,279,612.26	642,744.47	4,670,195.65
4,200,602.43	171,360.06	4,780,443.33
3,246,551.64	4,041,022.28	3,705,989.32
3,354,285.69	4,620,340.66	2,833,346.14

DELTA X = X-WGS84(ITRF2014)- (X-ETRF2000)

DELTA Y= Y- WGS84(ITRF2014)- (Y-ETRF2000)

DELTA Z= Z-WGS84(ITRF2014) – (Z-ETRF2000)

DELTA X	DELTA Y	DELTA Z
(METERS)	(METERS)	(METERS)
-537.06	485.99	228.69
-0.54	0.57	0.42
-0.48	0.56	0.42
-0.90	0.41	0.30
-0.91	0.41	0.30

7. When dealing with points in Europe, the task is to convert ETRF2000 geocentric Cartesian coordinates (X, Y, Z) into ETRF2000 latitude, longitude, and ellipsoidal height. Additionally, three more columns need to be added to the XLS table. These additional columns should indicate the accuracy of the coordinates in meters, specifying the number of decimal digits. You can utilize the useful tool provided by NOAA (<https://geodesy.noaa.gov/NCAT/>) for this purpose.

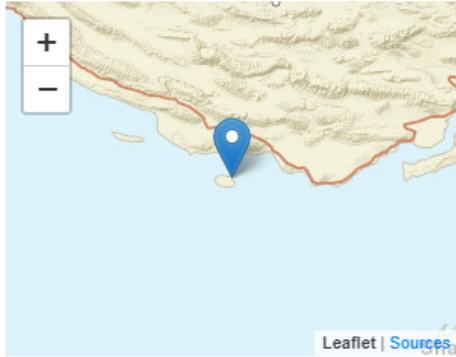
X-ETRF2000	Y-ETRF2000	Z-ETRF2000
(METERS)	(METERS)	(METERS)
3,149,486,460.06	597,043,777.01	5,495,632,208.31
4,279,612.26	642,744.47	4,670,195.65
4,200,602.43	171,360.06	4,780,443.33
3,246,551.64	4,041,022.28	3,705,989.32
3,354,285.69	4,620,340.66	2,833,346.14

Convert/Transform from:

Horizontal

Horizontal+height

XYZ



X (m)

Y (m)

Z (m)

Input reference frame (historically called 'horizontal datum')

*Don't see a reference frame in the list? Click here to learn more.*

SPC zone

Output (his dat)

**Submit**

**Converted Coordinate**

Reference Frame:

Lat-Lon-Height		SPC		UTM/USNG		XYZ (m)	
Latitude	N26° 32' 46.95983" N263246.95983 26.5463777309	Zone	N/A	Zone	<input type="text" value="40"/>	X	3,354,285.690
Longitude	E54° 01' 15.64768" E0540115.64768 54.0210132443	Northing	N/A (m) N/A (usft) N/A (ift)	Northing (m)	2,939,644.625	Y	4,620,340.660
Ellipsoid Height (m)	N/A	Easting	N/A (m) N/A (usft) N/A (ift)	Easting (m)	203,181.711	Z	2,833,346.140
		Convergence (dms)	N/A	Convergence (dms)	-01 19 56.46		
		Scale factor	N/A	Scale factor	1.00068785		
		Combined factor	N/A	Combined factor	1.00068658		
				USNG	40RBQ0318239645		

*You may change the default UTM zone. The change is processed interactively once a lat-long is converted; DO NOT click the Submit button.*

	Lat-ETRF2000	Long-ETRF2000
Point 2	47.37225648	8.541274549
Point 3	48.86118742	2.33603809
Point 4	35.74479756	51.22165343
Point 5	26.54637773	54.02101324

## Conclusion

Throughout this exercise, we have covered fundamental theoretical concepts and practical tools that are crucial for spatial professionals in effectively handling conversions and transformations between different coordinate reference systems and data. We have explored the differences between Cartesian, curvilinear, and projection coordinates in relation to various geodetic data. Additionally, we have provided practical solutions for performing the required coordinate conversions and transformations. Furthermore, we have discussed the computational procedure for converting between orthometric and ellipsoidal heights, particularly when geoid undulations are not referenced to a regional ellipsoid.

## Exercise 3: Spectral Indexes

### Introduction:

A spectral index is a mathematical formula that operates on different spectral bands of an image at each pixel. The widely used formula is the normalized difference (ND), which calculates the difference between two specific bands and normalizes it by their sum

$$ND = \frac{B_1 - B_2}{B_1 + B_2} \quad -1 \leq ND \leq 1$$

The Normalized Difference Vegetation Index (NDVI) is a widely used spectral index in remote sensing and vegetation studies. It is designed to quantify and analyze the density and health of vegetation cover across a given area. NDVI provides valuable insights into vegetation dynamics, plant growth, and ecosystem health, making it an essential tool for various applications such as agriculture, forestry, and environmental monitoring.

The calculation of NDVI involves the use of near-infrared (NIR) and red spectral bands, typically obtained from satellite or aerial imagery. The formula for NDVI is as follows:

$$NDVI = (NIR - Red) / (NIR + Red)$$

The near-infrared band reflects strongly from healthy vegetation, while the red band is absorbed by chlorophyll in the plants. By comparing the reflectance values of these two bands, NDVI calculates a value ranging from -1 to 1. The resulting NDVI values represent the density and vigor of vegetation, with higher values indicating healthier and more abundant vegetation.

### Key Features and Interpretation of NDVI:

**Vegetation Density:** NDVI provides a measure of the amount of vegetation present in an area. Higher NDVI values correspond to denser vegetation cover, while lower values indicate sparse or bare areas.

**Plant Health:** NDVI is sensitive to changes in plant health and stress. It can detect variations in vegetation vigor, such as drought stress, nutrient deficiencies, disease outbreaks, or damage caused by pests.

**Land Cover Classification:** NDVI is used to differentiate between various land cover types. It helps in distinguishing forests, croplands, grasslands, and urban areas based on their distinctive NDVI signatures.

**Phenological Studies:** NDVI is instrumental in monitoring seasonal changes in vegetation growth and phenology. It aids in tracking the timing of plant development, leaf emergence, flowering, and senescence.

**Environmental Monitoring:** NDVI is employed to assess the impact of environmental factors on vegetation, such as temperature, moisture levels, pollution, and land degradation. It contributes to monitoring ecosystem health, biodiversity, and land-use changes.

The versatility and simplicity of NDVI make it a valuable tool for researchers, land managers, and policymakers. Its widespread adoption in various disciplines highlights its significance in understanding vegetation dynamics, managing natural resources, and addressing global challenges like food security, climate change, and sustainable land use.

The objective of this exercise is to analyze a combined (median) image derived from Sentinel 2 Surface Reflectance images within a designated area of interest (AOI) over a specified time period. The aim is to identify and quantify the extent of areas (pixels) with healthy vegetation, characterized by an NDVI (Normalized Difference Vegetation Index)  $> 0.3$ .



# A planetary-scale platform for Earth science data & analysis

Earth Engine's public data archive includes more than forty years of historical imagery and scientific datasets, updated and expanded daily.

[View all datasets](#)

<https://developers.google.com/earth-engine/datasets>



Sentinel-2 MSI: Multispectral Instrument





## Surface Reflectance

Level-2A orthorectified atmospherically corrected surface reflectance.

**Dataset availability:** 2017-03-28 – Present

## Harmonized Sentinel-2 MSI: MultiSpectral Instrument, Level-2A



### Dataset Availability

2017-03-28T00:00:00Z–2023-06-19T12:57:28

### Dataset Provider

[European Union/ESA/Copernicus](#)

### Earth Engine Snippet

```
ee.ImageCollection("COPERNICUS/S2_SR_HARMONIZED")
```



### Tags

After selecting a suitable location (Abbas abad, Iran), we should follow the steps below:

Access the collection of Sentinel-2 Level-2A (Surface Reflectance) data by visiting the provided link:

([https://developers.google.com/earth-engine/datasets/catalog/COPERNICUS\\_S2\\_SR\\_HARMONIZED](https://developers.google.com/earth-engine/datasets/catalog/COPERNICUS_S2_SR_HARMONIZED)).

Apply filters to the collection to narrow down the data. Specifically, filter the data to include only the time period from September 1, 2020, to December 31, 2020, and focus on the geographical area of Abbas abad, Iran (approximately located at coordinates:48.85, 38.38). Additionally, filter the data based on cloud coverage. To accomplish this, use the following filtering operations:

Use the `filterDate('start', 'end')` function to specify the desired date range.

Use the `filterBounds(geometry)` function to define the area of interest, in this case, Abbas abad, Iran

Apply the `filter(ee.Filter.condition('property', value))` method to filter the collection based on the cloud property.

Next, implement the radiometric scaling factor to all the images within the filtered collection. To do this, iterate over the collection using the `map` function.

Google Earth Engine

Search places and datasets...

Scripts Docs Assets

Filter scripts... NEW

Owner (1)  
users/salaritekmehdashi2055456/EX03  
EX03  
EX3.2  
ex6  
karoon  
Writer  
No accessible repositories. Click Refresh to check

EX3.2 \*  
Imports (1 entry)  
var geometry: Point (48.85, 38.38)  
1  
2 // step 1  
3 var sentinel\_s2 = ee.ImageCollection("COPERNICUS/S2\_SR\_HARMONIZED");  
4 // step 1  
5 var ST2\_imgage\_coll = ee.ImageCollection("COPERNICUS/S2\_SR\_HARMONIZED")  
6  
7 // step 2  
8 var ST2\_filtered = ST2\_imgage\_coll.filterDate('2020-03-01', '2021-07-01')  
9 filterBounds(geometry)  
10

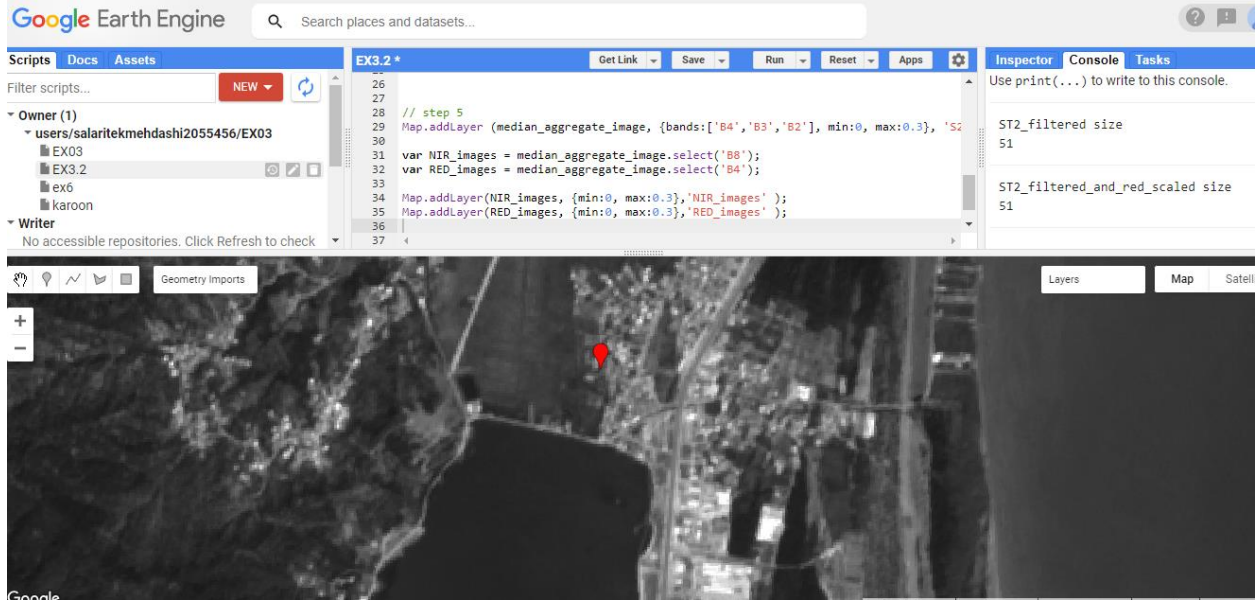
Inspector Console Tasks  
Use print(...) to write to this console.  
ST2\_filtered size  
51  
ST2\_filtered\_and\_red\_scaled size  
51

Geometry Imports

Abas Abad  
شهرک عباس آباد  
Rasht-Asfara Rd  
Majid Housh (house)  
Ti Reza

Map Sat

Keyboard shortcuts Map data ©2023 200 m



Use the `ee.Reducer.median()` function to merge the images in the refined collection, while specifically selecting the Red (R), Green (G), Blue (B), and Near-Infrared (NIR) bands.

Calculate the Normalized Difference Vegetation Index (NDVI) on the merged image, which has undergone radiation adjustments. To compute the NDVI, subtract the RED band from the NIR band, and divide the result by the sum of the NIR and RED bands, both chosen from the image.

Assign a descriptive label by renaming the band of the NDVI image.

Use the `Map.addLayer` method to visually represent the RGB image (true color composite), the NIR band, and the NDVI index.

Display a false-color layer by utilizing the NIR, red, and green bands for RGB. This color scheme assigns a distinct red color to all pixels containing vegetation, making them easily distinguishable from their surroundings to the human eye.

Google Earth Engine

Search places and datasets...

Scripts Docs Assets

Filter scripts... NEW

Owner (1)  
users/salaritekmehdashi2055456/EX03  
EX03  
EX3.2  
ex6  
karoon

Writer  
No accessible repositories. Click Refresh to check again.

Reader  
No accessible repositories. Click Refresh to check again.

```

31 var NIR_images = median_aggregate_image.select('B8');
32 var RED_images = median_aggregate_image.select('B4');
33
34 Map.addLayer(NIR_images, {min:0, max:0.3}, 'NIR_images');
35 Map.addLayer(RED_images, {min:0, max:0.3}, 'RED_images');
36
37 var numerator = NIR_images.subtract(RED_images);
38 var denominator = NIR_images.add(RED_images);
39
40 var NDVI = numerator.divide(denominator);
41 NDVI = NDVI.rename('NDVI');
42 print('NDVI', NDVI);
43 Map.addLayer(NDVI, {min:-1, max:1}, 'NDVI');
44
45
46

```

Inspector Console Tasks

Pixels

S2\_median\_aggregate\_image true color composite RGB:

geometry (1 pt) Editing: Drag to move point. Delete Exit

Layers Map Satellite

Scripts Docs Assets

Filter scripts... NEW

Owner (1)  
users/salaritekmehdashi2055456/EX03  
EX03  
EX3.2  
ex6  
karoon

Writer  
No accessible repositories. Click Refresh to check again.

```

40 var NDVI = numerator.divide(denominator);
41 NDVI = NDVI.rename('NDVI');
42 print('NDVI', NDVI);
43 Map.addLayer(NDVI, {min:-1, max:1}, 'NDVI');
44
45 // step 7,8
46
47 // Red is represented in NearInfraRed
48 // Green is represented in Red
49 // Blue is represented in Green
50 Map.addLayer(median_aggregate_image, {bands:['B8','B4','B3'], min
51
52

```

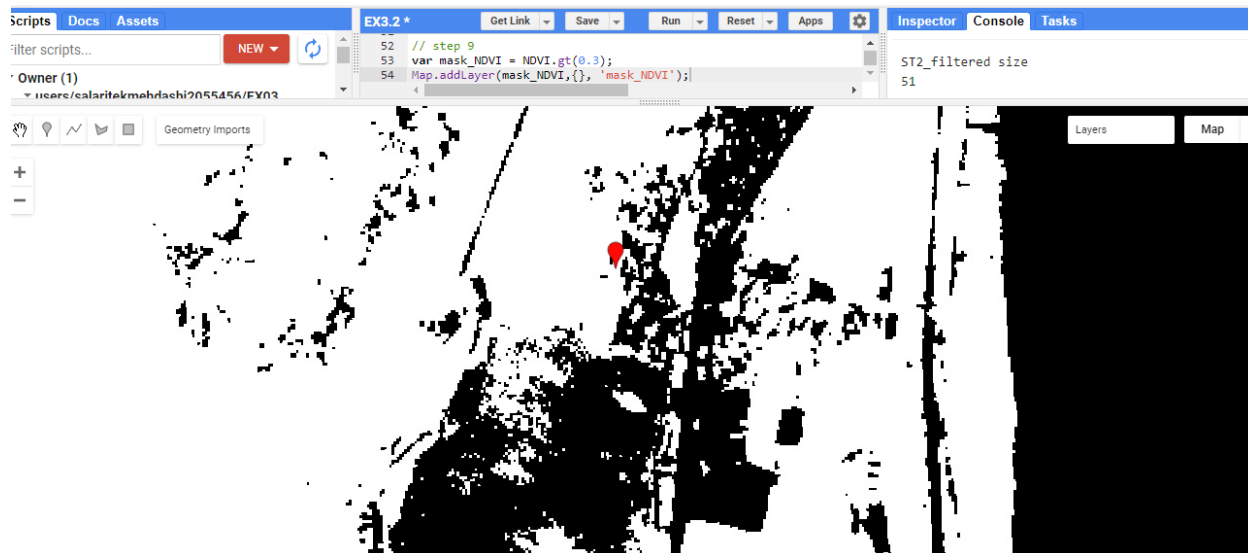
Inspector Console Tasks

S2\_median\_aggregate\_image true color composite RGB:

geometry (1 pt) Editing: Drag to move point. Delete Exit

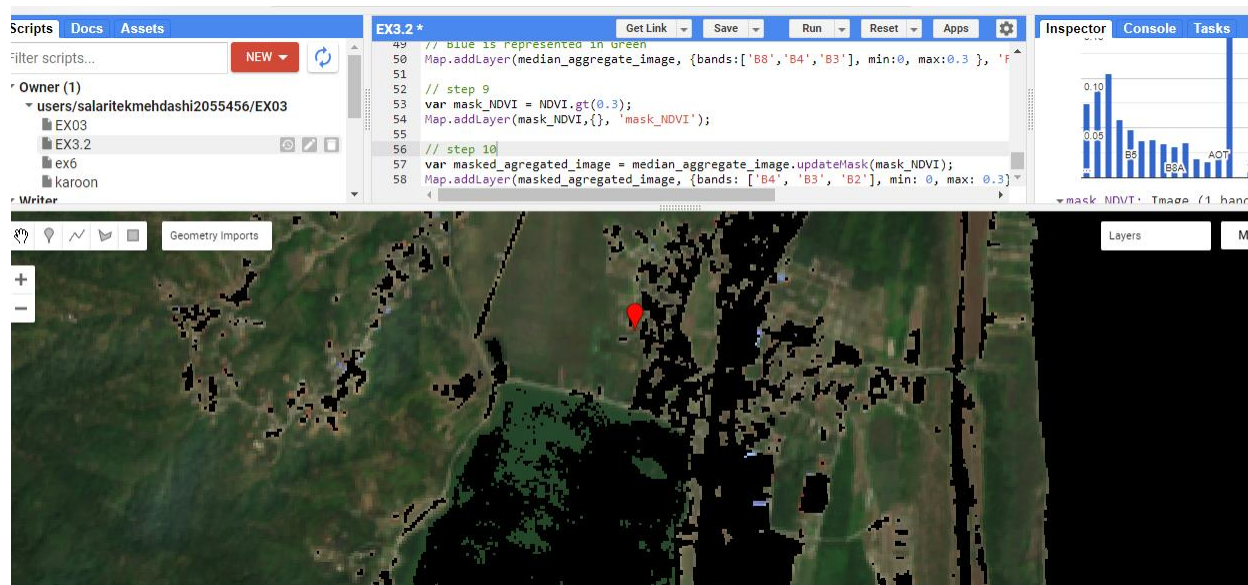
Layers Map Satellite

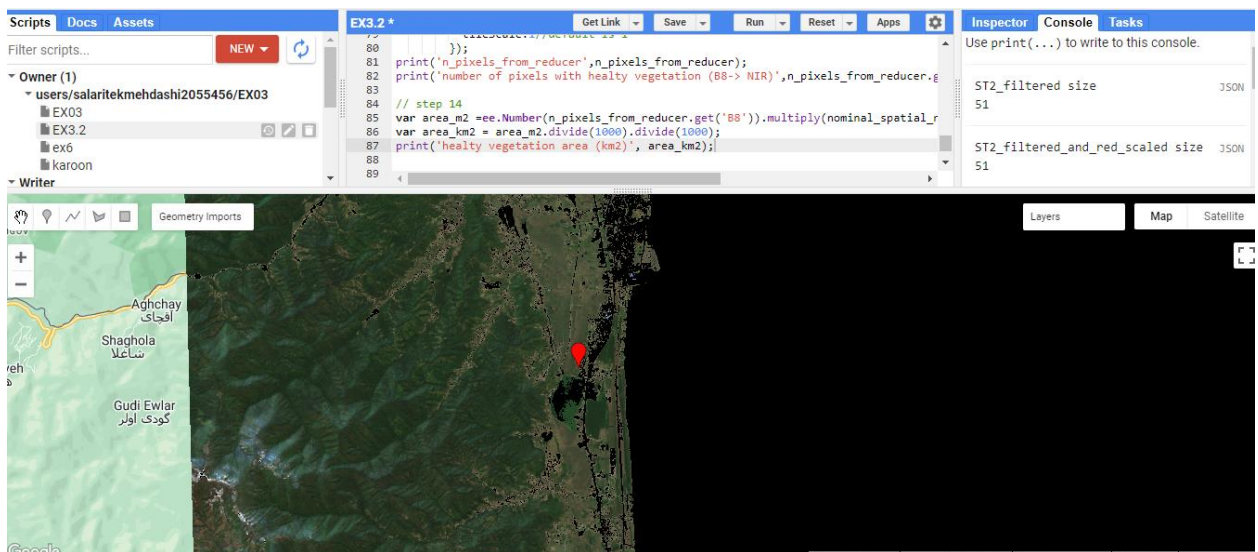
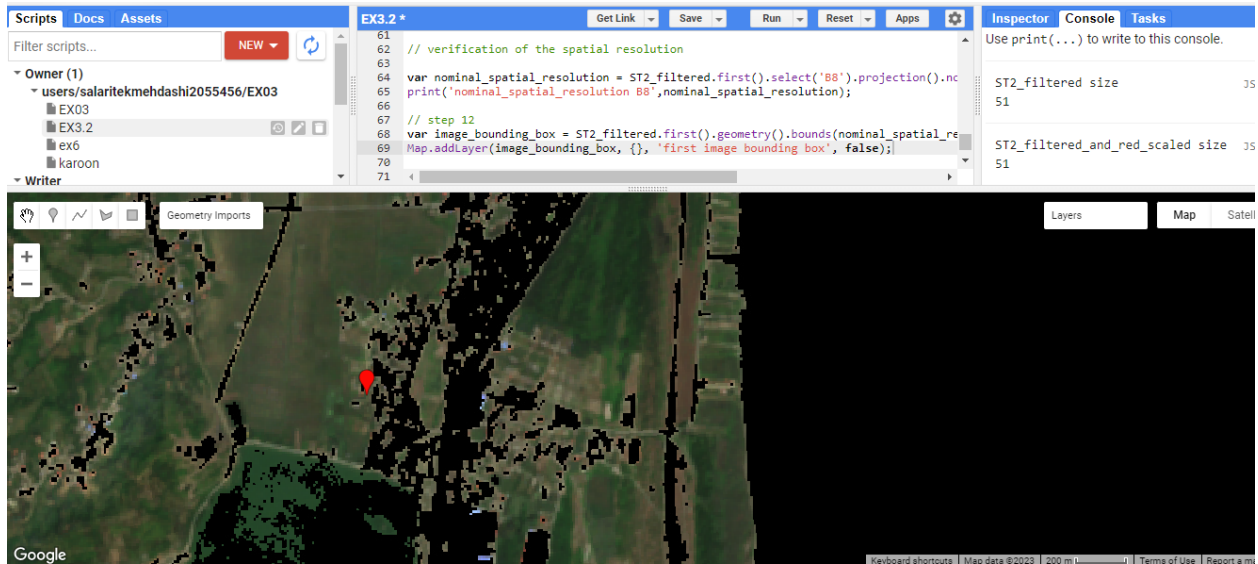




Now we should generate a mask to distinguish pixels with healthy vegetation by setting a threshold on the NDVI values using the gt method. In this situation, the threshold is defined as  $NDVI > 0.3$ .

Then we need to apply the previously created mask to identify and extract the regions with healthy vegetation from the original image. Use the updateMask method to apply the mask, resulting in pixels with NDVI values less than or equal to 0.3 becoming transparent and being excluded from further calculations.





## Conclusion:

The use of NDVI facilitates remote sensing applications in part because it correlates with the status of a broad array of vegetation properties, thus simplifying the complex. At the same time, popular development of remote sensing technology has subsequently promoted the generation of low-cost image data helpful for broadening NDVI applications. Remote sensing has changed the way the land resources are viewed, used, and managed. The same applies toward how NDVI is implicated with vegetation health, patterns, and status. There is no doubt that NDVI

will continue to be a dominant vegetation index, but the effective use of NDVI depends on the quality of multispectral data and the interpretation of NDVI values. The analysis of NDVI values provides a powerful tool to monitor vegetation, allowing us to obtain crucial insights into vegetation health, land cover changes, agricultural productivity, and the effects of climate change. By leveraging NDVI-based assessments, we can effectively intervene in a timely manner in areas such as agriculture, land management, and conservation efforts. The utilization of remote sensing technology and the careful analysis of NDVI data enable us to enhance our comprehension of ecosystems, empowering us to make well-informed decisions that promote the sustainable utilization of natural resources and bolster resilience in the face of environmental challenges. This comprehensive approach enables us to strive towards a more sustainable and harmonious coexistence with our natural environment.

<https://code.earthengine.google.com/0151639d31a5188e62c4d5b06b7d90fa>



## Exercise 05:

### Flood mapping with SAR

Flood mapping using Synthetic Aperture Radar (SAR) is effective for monitoring and assessing floods. SAR utilizes microwave signals for all-weather and day-and-night imaging. SAR has advantages like penetrating cloud cover and capturing backscatter signals to identify flooded areas. SAR-based flood mapping involves comparing SAR data before and after floods to observe changes in backscatter intensity. Various algorithms are used to distinguish flooded areas. SAR-based flood mapping provides valuable information for assessing flood severity, planning response actions, and improving flood forecasting and early warning systems. Combining SAR data with other geospatial information enhances flood mapping accuracy and provides insights into flood impacts on the environment and infrastructure. Remote sensing, using both optical and Synthetic Aperture Radar (SAR) satellite imagery, has great potential in detecting flooded areas. However, cloud cover during flood events hinders the effectiveness of passive optical remote sensing. SAR remote sensing, on the other hand, can penetrate clouds and provide all-weather capabilities, making it highly valuable for flood detection. In rural areas, SAR backscatter intensity accurately identifies flooded areas, making SAR imagery an essential tool for flood mapping. SAR data has a temporal resolution of 6-12 days, with a precise 6-day repeat cycle at the equator when data from both Sentinel-1A and Sentinel-1B satellites are utilized.

In conclusion, it is a powerful tool for monitoring floods, overcoming cloud cover limitations, and providing essential information for flood response, forecasting, and understanding flood impacts.

### Polarization in SAR

Polarization in Synthetic Aperture Radar (SAR) pertains to the alignment of electromagnetic waves emitted and received by the radar system. SAR systems have the capability to transmit and receive signals in various polarization modes, offering valuable insights into the characteristics of observed targets.

There are four main polarization modes commonly used in SAR:

Single polarization (HH or VV): In this mode, the SAR system uses a single polarization, either horizontal (HH) or vertical (VV), for transmitting and receiving waves. Single polarization is useful for general imaging purposes, providing basic information about the backscattered energy from the targets.

Dual polarization (HH/VV or HV): Dual polarization mode involves the transmission and reception of waves in two orthogonal polarizations. For instance, HH/VV represents horizontal transmit and receive (HH) polarization paired with vertical transmit and receive (VV) polarization. HV polarization signifies horizontal transmit with vertical receive. Dual polarization enhances the information content of SAR data and enables better differentiation between different types of targets such as vegetation, buildings, and water bodies.

Quad polarization (HH/HV/VH/VV): Quad polarization, also known as full polarization or fully polarimetric mode, employs all four possible combinations of horizontal (H) and vertical (V) polarizations for transmitting and receiving waves. This mode provides comprehensive information about the scattering properties of targets, facilitating detailed analysis and classification of different target types. Quad polarization is particularly valuable for applications like land cover classification, forest monitoring, and soil moisture estimation.

Compact polarization (e.g., HH+HV, VV+VH): Compact polarization mode combines two different polarizations into a single channel. For example, HH+HV denotes the combination of horizontal transmit and receive (HH) polarization with horizontal transmit and vertical receive (HV) polarization. Compact polarization strikes a balance between data complexity and the amount of information derived from SAR data.

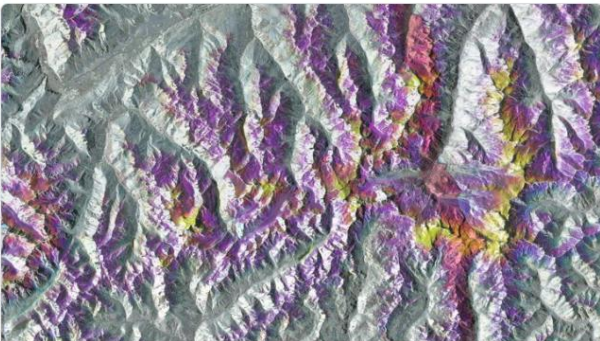
By utilizing diverse polarization modes, SAR systems capture additional information about targets, such as their scattering mechanisms, surface roughness, orientation, and dielectric properties. This diversity in polarization enables a wide range of applications across various fields, including agriculture, forestry, hydrology, geology, and disaster monitoring.

## Introduction

The objective of this exercise is to utilize Google Earth Engine to map a flooding event that occurred a few weeks ago in the Alborz province in Iran. (the pictures will be attached in the last page of this exercise) The analysis focuses on SAR (Synthetic Aperture Radar) imagery captured by the Sentinel-1 satellite. One challenge with this type of imagery is the presence of significant noise, which will be addressed by applying a dedicated filter to remove it.

There are 2 image collections in SAR data and we are going to use the second one.

1. ee.ImageCollection COPENICUS/S1 GRD FLOAT
2. ee.ImageCollection COPENICUS/S1 GRD



Sentinel-1 SAR GRD: C-band Synthetic Aperture Radar

**Data availability:** 2014 – Present

The Sentinel-1 mission provides data from a dual-polarization C-band Synthetic Aperture Radar (SAR) instrument. SAR instruments are capable of acquiring meaningful data in all weather conditions (even clouds) during daytime and

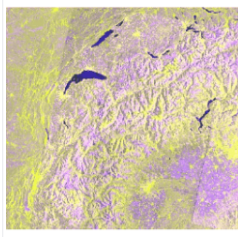


Sentinel-2 MSI: Multispectral Instrument

**Data availability:** 2015 – Present

The Sentinel-2 mission collects high-resolution multispectral imagery useful for a broad range of applications, including monitoring of vegetation, soil and water cover, land cover change, as well as humanitarian and disaster risk.

## Sentinel-1 SAR GRD: C-band Synthetic Aperture Radar Ground Range Detected, log scaling



### Dataset Availability

2014-10-03T00:00:00Z–2023-06-24T13:50:59

### Dataset Provider

[European Union/ESA/Copernicus](#)

### Earth Engine Snippet

```
ee.ImageCollection("COPERNICUS/S1_GRD")
```



### Tags

[copernicus](#) [esa](#) [eu](#) [radar](#) [sar](#) [sentinel](#) [backscatter](#) [polarization](#)

This dataset consists of all the GRD scenes, each characterized by one of three different resolutions (10, 25, or 40 meters), four bands representing different polarizations, and three instrument modes. To utilize this collection in a mosaic context, it is recommended to filter and select a consistent set of bands and parameters to ensure homogeneity.

We pre-process each scene following these steps:

1. Thermal noise removal: The effect of moisture is mitigated by removing thermal noise from the scene.
2. Radiometric calibration: The scene undergoes radiometric calibration to ensure consistent measurements of the radar backscatter.
3. Terrain correction: For areas with available data, SRTM 30 or ASTER DEM is used to perform terrain correction. While it may not completely eliminate the effects of topography, it helps reduce them. In areas beyond 60 degrees' latitude where SRTM data is unavailable, ASTER DEM is used.

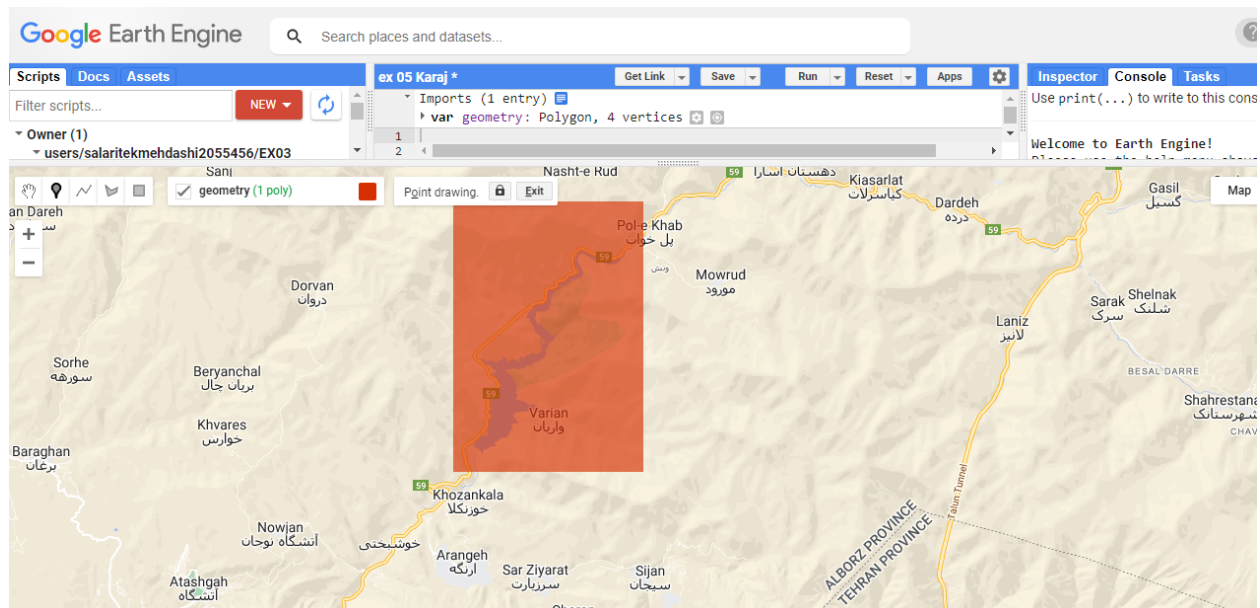
The resulting terrain-corrected values are then converted to decibels using log scaling ( $10 \cdot \log_{10}(x)$ ). This quantity is referred to as Sigma-nought ( $\sigma_0$ ), which represents the radar backscatter coefficient and serves as a conventional measure of radar signal strength reflected by a distributed scatterer. Typical values for sigma-nought range from -30 dB to 0 dB.

The polarizations HH (horizontal transmit and horizontal receive) and VV (vertical transmit and vertical receive) are used in the analysis. Since polar regions are not being analyzed in this case, only these two polarization bands are considered.

The decision to utilize Radar imagery for flood monitoring is based on its ability to overcome the limitations posed by cloud cover, unlike optical imagery. SAR images are not affected by the presence of clouds, enabling consistent observations during flood events.

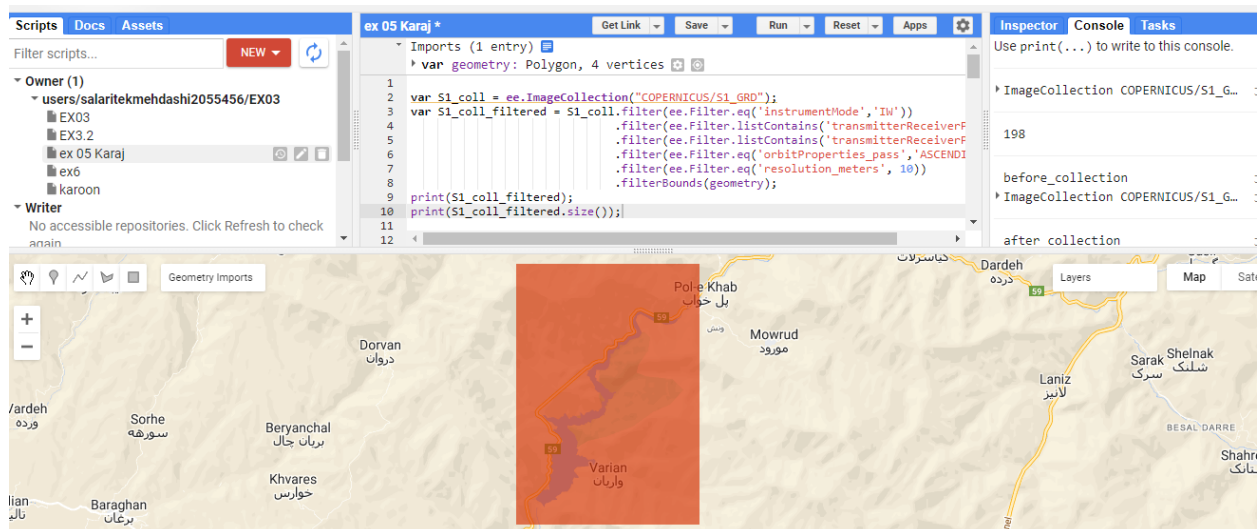
These SAR images are capable of detecting the presence of water by comparing areas before and after the flood, providing insights into the magnitude of the flood. The VH band (vertical transmit and horizontal receive) is particularly sensitive to the presence of water and is used for radar detection.

The initial step in the process is to define the specific area of study. One approach is to utilize a tool provided by FAO (Food and Agriculture Organization) to identify a specific administrative territory, which helps in focusing the analysis on the desired region.



To filter the collection of metadata for different parameters, the following criteria should be considered:

1. Instrument operational mode: Select the desired mode, which in this case is IW (Interferometric Wide Swath).
2. Polarization: Choose the VH and VV polarizations to compute a false color composite.
3. Orbits: Select the ascending orbit for the desired data.
4. Geometry: Apply the Area of Interest (AOI) for the specific region of interest.
5. Resolution: Opt for the best resolution available, which is 10 meters. Note that the resolution information is stored as a DOUBLE value, not a STRING.



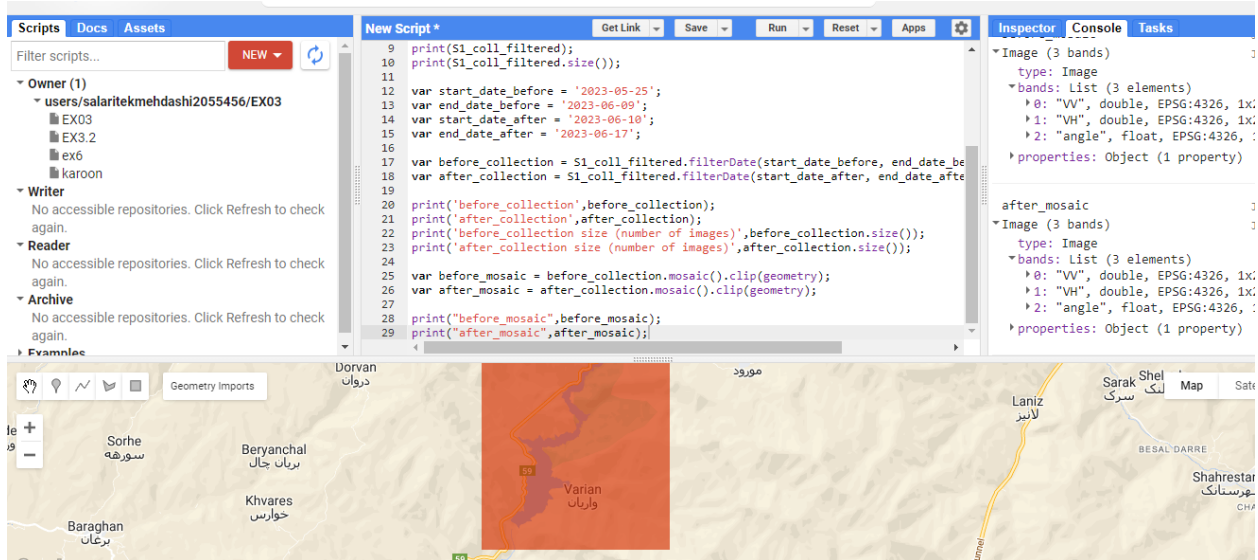
To obtain the aggregated image for the period before the flooding and the period after the flooding, you can define the following date ranges:

Period before the flooding: Starting date: May 25, 2023 Finishing date: June 09, 2023

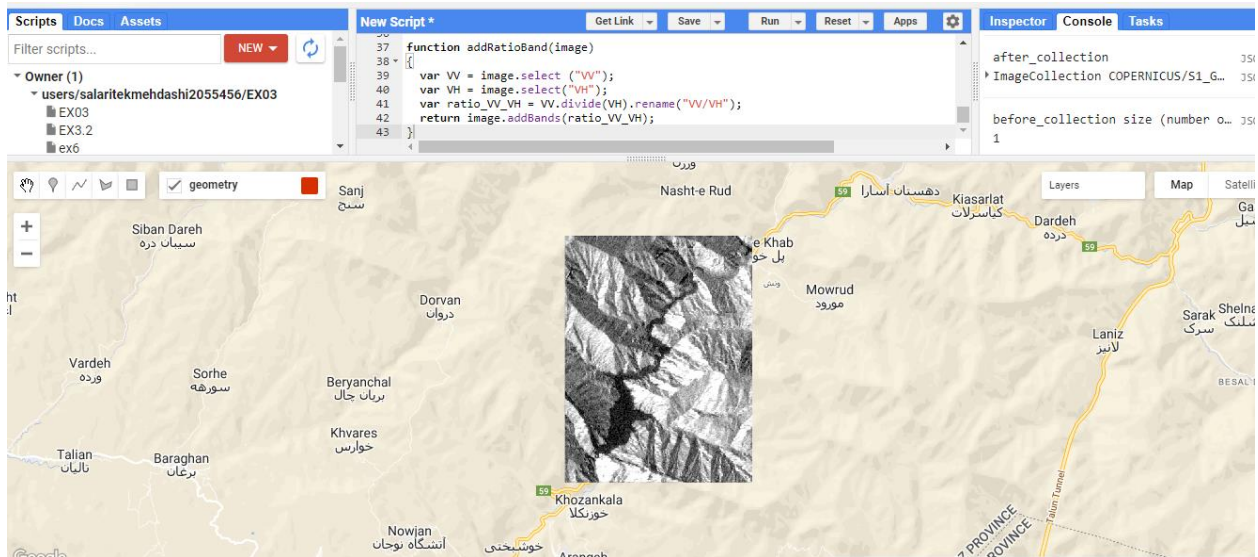
Period after the flooding: Starting date: June 10, 2023 Finishing date: June 17, 2023

Using these date ranges, you can aggregate the SAR imagery for the respective periods and compare them to observe the differences in the areas affected by the flooding.





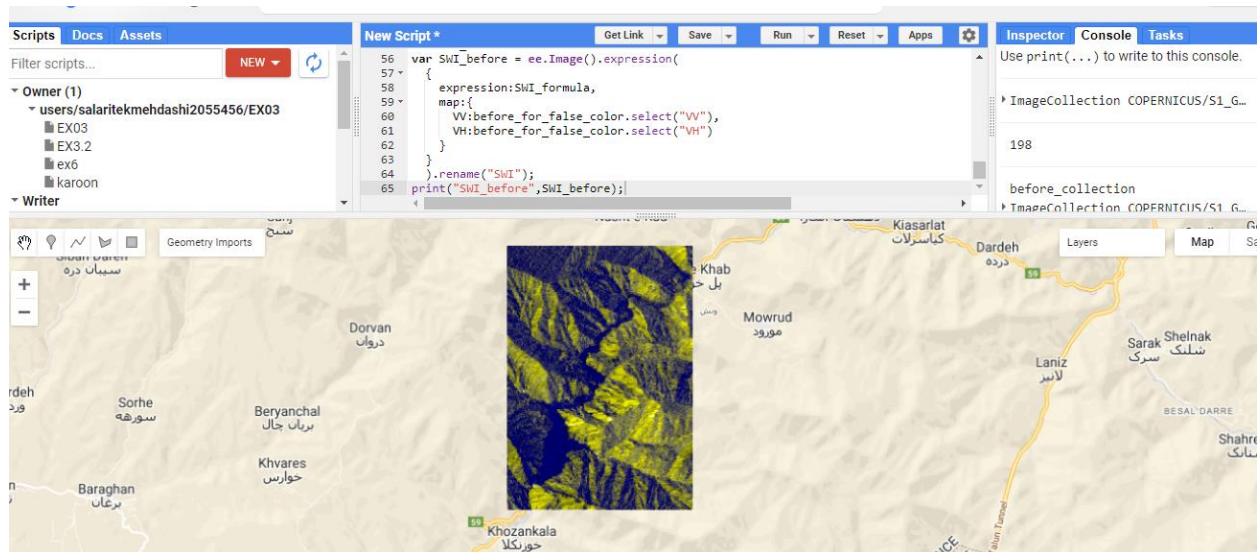
Considering that water is represented by black pixels in radar images, you can easily observe a higher presence of water in the image taken after the flooding event. This contrast between the before and after images allows for a clear visualization of the areas that have been affected by the flood, as they would appear darker in the post-flooding image.



To visualize SAR imagery in a false color composite, we can assign different bands or polarizations to the red, green, and blue channels, respectively. This technique enhances the interpretation of the data and allows us to distinguish various features and phenomena.

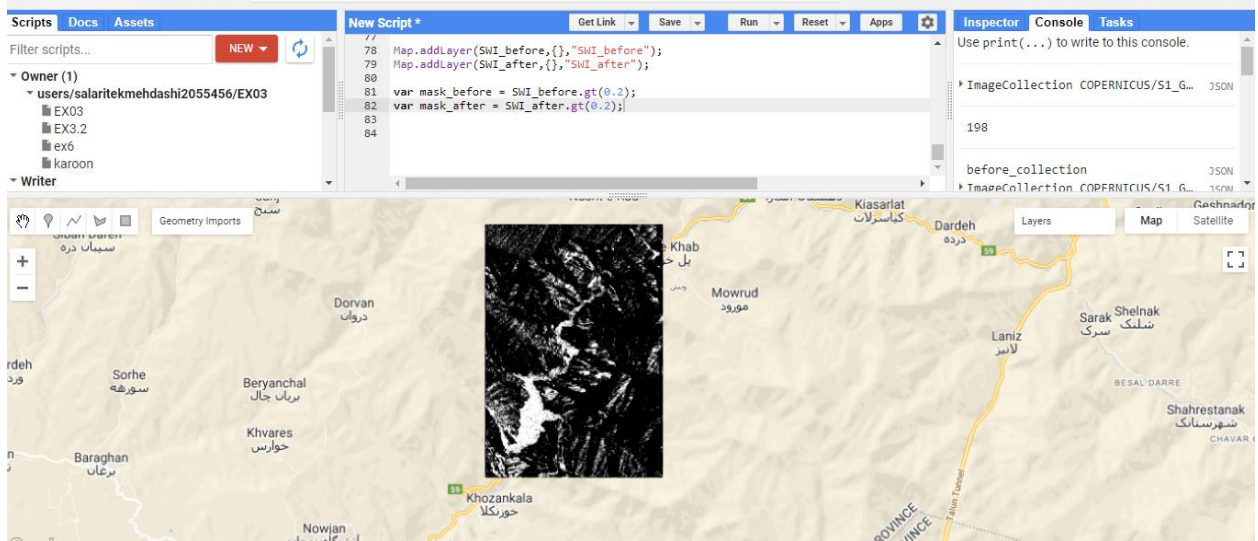
In the case of SAR imagery, we can use the VH (vertical transmit and horizontal receive) polarization for the red channel, the VV (vertical transmit and vertical receive) polarization for the green channel, and the HH (horizontal transmit and horizontal receive) polarization for the blue channel. This combination provides a visually appealing representation of the data.

By displaying the SAR imagery in a false color composite, we can observe different characteristics of the scene, such as the backscatter intensity and the distribution of targets with varying scattering properties. This visualization technique aids in the interpretation and analysis of SAR data for various applications, including flood mapping, land cover classification, and change detection.

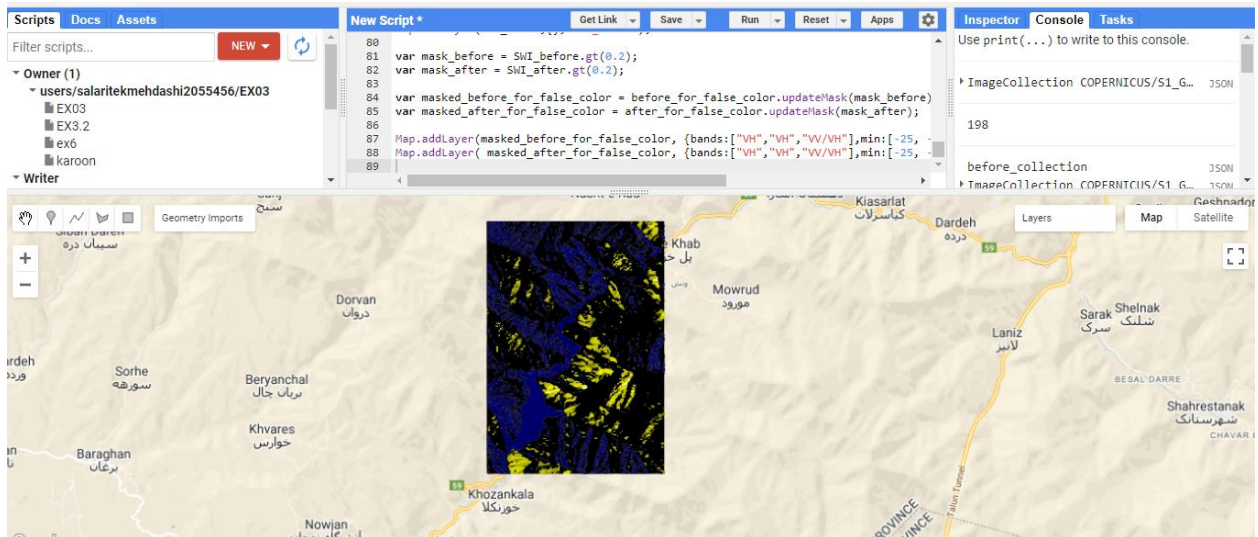


In this step we use SWI for flood mapping.

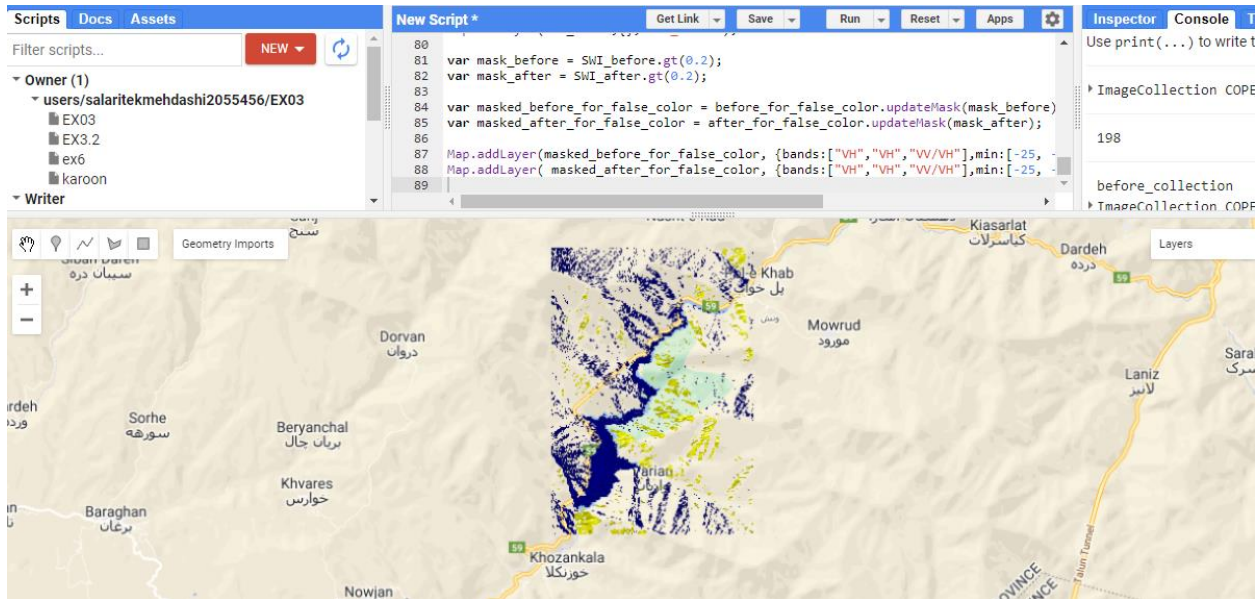




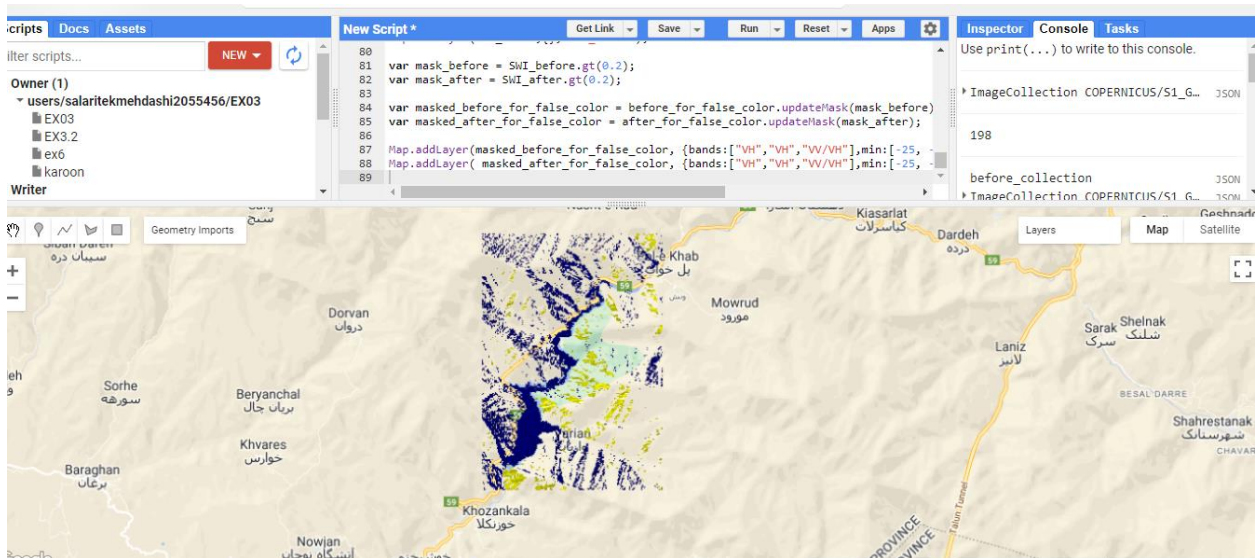
Here we should apply the masked false color, by applying the masks to the false color composite, you can effectively highlight the areas affected by the flood and visually compare the changes between the "before" and "after" periods.



Before:



After:



By the way of conclusion, SAR flood mapping is a valuable and effective tool for mapping and monitoring floods, offering essential information that supports decision-making, emergency response, and flood risk management. By integrating SAR flood mapping into existing flood management frameworks, we can enhance resilience, minimize losses, and improve disaster preparedness in regions prone to



flooding. This technology plays a crucial role in mitigating the impacts of floods and ensuring the safety and well-being of communities affected by such events.

<https://code.earthengine.google.com/807e210a39c2b602f4784f5c66e24717>







## Exercise 06:

### Classification of Remote Sensing imagery with Machine Learning algorithms

#### Machine Learning

Machine learning is a branch of [artificial intelligence \(AI\)](#) and computer science which focuses on the use of data and algorithms to imitate the way that humans learn, gradually improving its accuracy. Machine learning is an important component of the growing field of data science. Through the use of statistical methods, algorithms are trained to make classifications or predictions, and to uncover key insights in data mining projects

#### Clustering:

Using unsupervised learning, clustering algorithms can identify patterns in data so that it can be grouped. Computers can help data scientists by identifying differences between data items that humans have overlooked.

**Supervised Learning:** In this approach, the machine learning model is trained on labeled data, where the input data is associated with corresponding output labels or target values. The model learns to map input data to output labels, enabling it to make predictions or classifications on new, unseen data.

**Unsupervised Learning:** This technique involves training the model on unlabeled data, where there are no predefined output labels or target values. The model learns to find patterns, structures, or relationships in the data without explicit

guidance. Clustering and dimensionality reduction are common applications of unsupervised learning.

**K-means Clustering:** It is one of the most commonly used clustering algorithms. It aims to partition the data into a predefined number of clusters, denoted by 'k'. The algorithm iteratively assigns data points to clusters based on their proximity to the cluster centroids, which are representative points within each cluster. The process continues until the cluster assignments stabilize.

## Introduction:

In this exercise, we will showcase the application of machine learning algorithms in Google Earth Engine (GEE) for classifying multispectral images obtained through remote sensing. The main objective is to determine the thematic class of each pixel by converting reflectance information into land cover classifications. Machine learning algorithms are highly effective when dealing with large datasets and can be applied for various purposes.

Specifically, our focus in this exercise is to classify individual pixels within a cloud-free composite of Landsat 7 data. This composite is created from raw Landsat 7 images, specifically capturing at-sensor radiance, collected within a defined area of interest (AOI) during a specific time period.

To initiate the process, we select the desired location and download the Landsat 7 raw (radiance) image collection from the Earth Engine Data Collection. Subsequently, we apply filtering based on factors such as date, location, and cloud coverage.

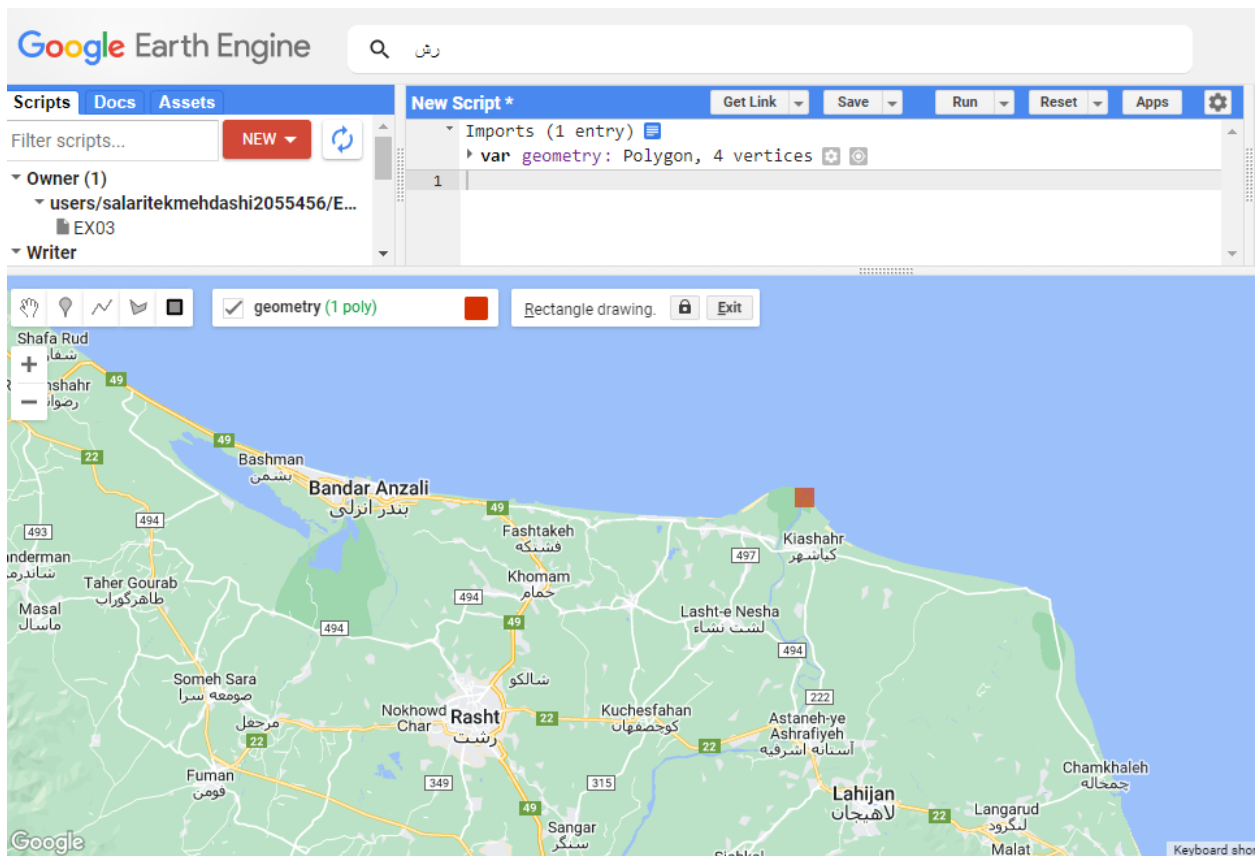
For this analysis, we will make use of the red, green, and blue color bands as the primary bands of interest. To generate a training dataset, we can create it within the designated region of interest (ROI).

## Chosen Area:

Sefid rood plain (Gilan province, Iran)

we need to generate a basic composite from a collection of raw Landsat images. To achieve this, we will utilize the `ee.Algorithms.Landsat.simpleComposite()` function, which has been developed by Google. This algorithm takes the input collection of raw Landsat scenes and applies Top of Atmosphere (TOA) calibration, aiming to minimize the impact of clouds as much as possible. Since our focus is on classifying land and not clouds, this step is crucial.

To begin, we should select the desired area and import the Landsat 7 dataset collection into the code editor of Google Earth Engine (GEE).



# A planetary-scale platform for Earth science data & analysis

Earth Engine's public data archive includes more than forty years of historical imagery and scientific datasets, updated and expanded daily.

[View all datasets](#)



Landsat 9 OLI-2/TIRS-2

2021–Present



Landsat 8 OLI/TIRS

2013–Present



Landsat 7 ETM+

1999–2021







### Surface Reflectance

Landsat 7 ETM+ Collection 2 atmospherically corrected surface reflectance.

**Dataset Availability:** January 1999–April 2022

Tier 1

Tier 2



### Top of Atmosphere

Landsat 7 ETM+ Collection 2 calibrated top-of-atmosphere (TOA) reflectance.

**Dataset Availability:** January 1999–April 2022

Tier 1

Tier 2



### Raw Images

Landsat 7 ETM+ Collection 2 DN values, representing scaled, calibrated at-sensor radiance.

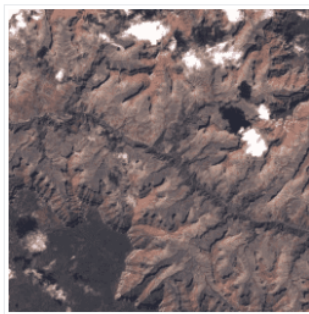
**Dataset Availability:** January 1999–April 2022

Tier 1

Tier 2

We use Raw Images because while we are using the composite we can decrease the effect of clouds a large quantity. Tier one has higher quality. Then we need to copy the link below into the google earth engine.

## USGS Landsat 7 Collection 2 Tier 1 Raw Scenes



### Dataset Availability

1999-05-28T01:02:17Z–2023-05-24T02:19:04

### Dataset Provider

[USGS](#)

### Earth Engine Snippet

```
ee.ImageCollection("LANDSAT/LE07/C02/T1")
```

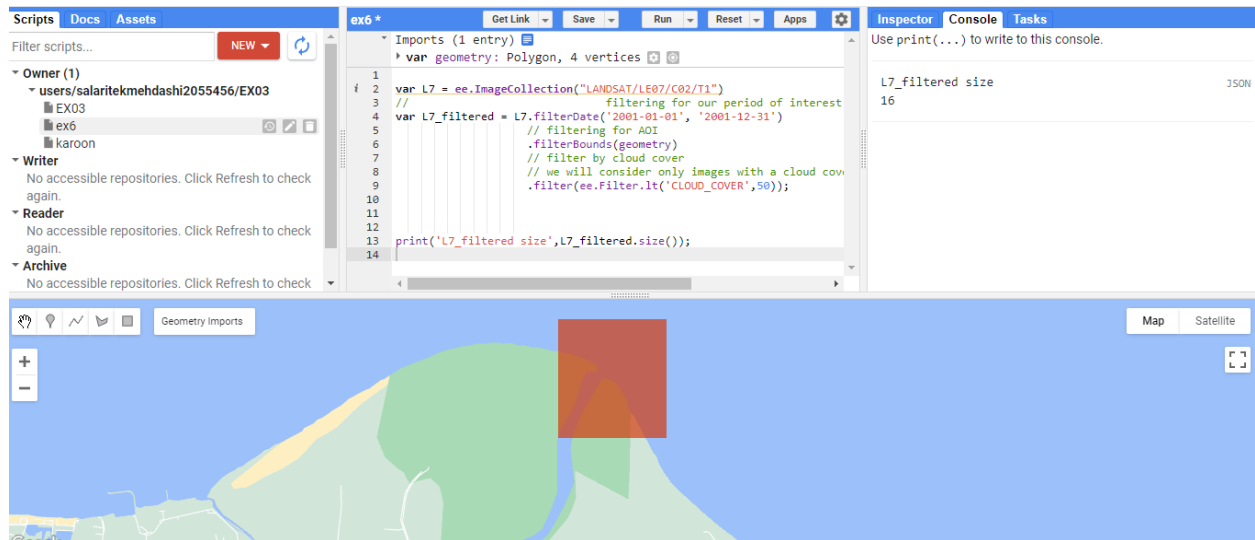


### Tags

c2 etm global l7 landsat le7 radiance t1 tier1 usgs

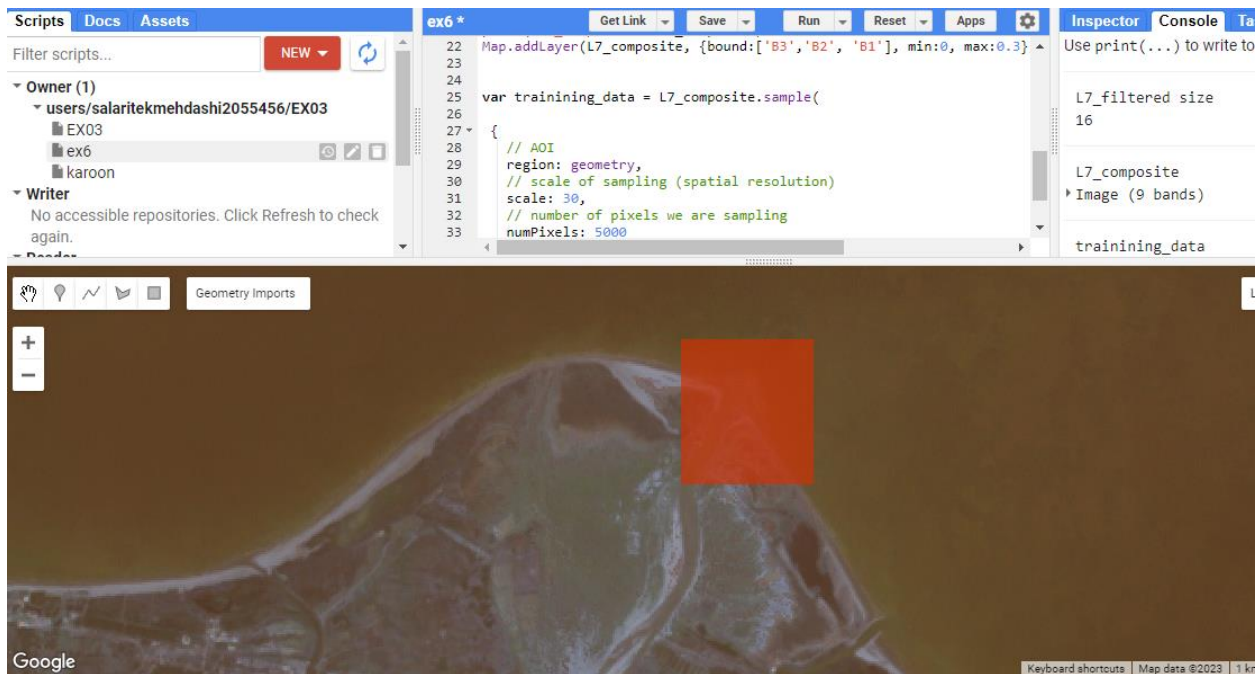
Afterwards, we proceed to filter the collection based on our desired time frame and the selected geometry. Specifically, we only consider images that have a cloud

cover of less than 50%. This information is available in the list of Image Properties. To verify if our code is written correctly, we should print it. We have 16 images.



We generate a single image that includes the information from 16 images, effectively aggregating them in a manner that minimizes the impact of clouds. The input for this process is the image collection, while the output is a single image. To achieve this, we utilize a dictionary and the `asFloat()` function to convert radiance values to Top of Atmosphere (TOA) reflectance within the range of 0 to 1. This process allows us to construct our input image, which will then be used in the classification algorithm.

Subsequently, we add the generated image as a layer to the map. Additionally, we can define visualization options to ensure the representation appears as a true color image. For reference, the Band tab on the Earth Engine Data Catalog provides information on the specific bands to use for each color channel (RGB: Red, Green, Blue; 03, 02, 01). In order to create our training dataset, we must generate a sample of pixels from the specific region we are interested in, taking into account the spatial resolution. It is crucial to prevent overfitting problems that can occur when using the entire dataset. Hence, we utilize a sampling method that necessitates a dictionary as an input, enabling us to carefully select the suitable pixels for training purposes.

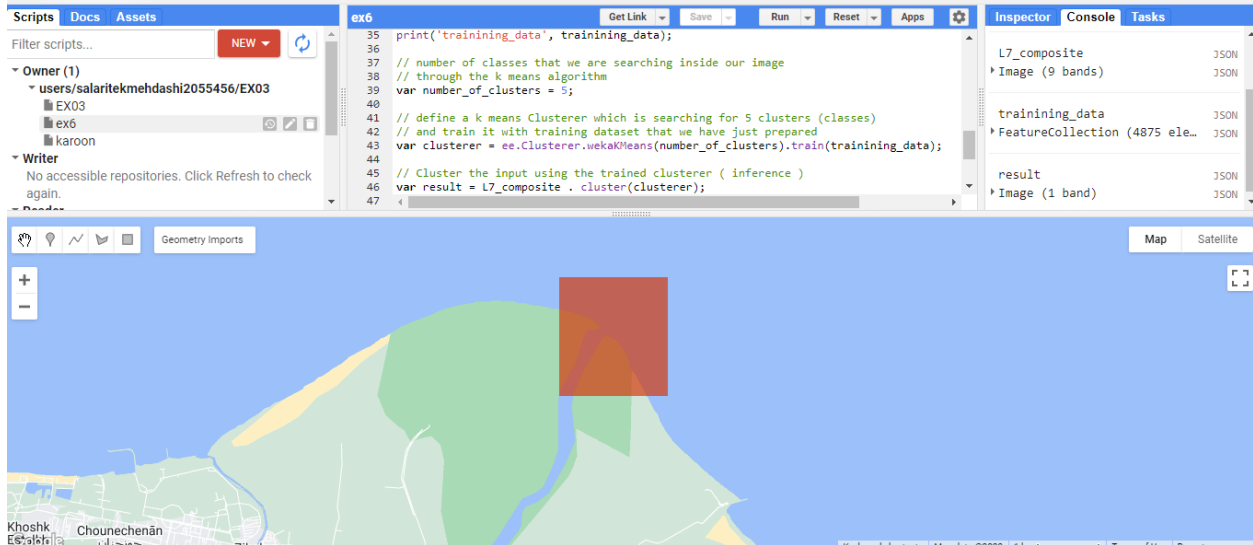


In an image classification problem, our objective is to categorize a given set of images into a specific number of predefined categories.

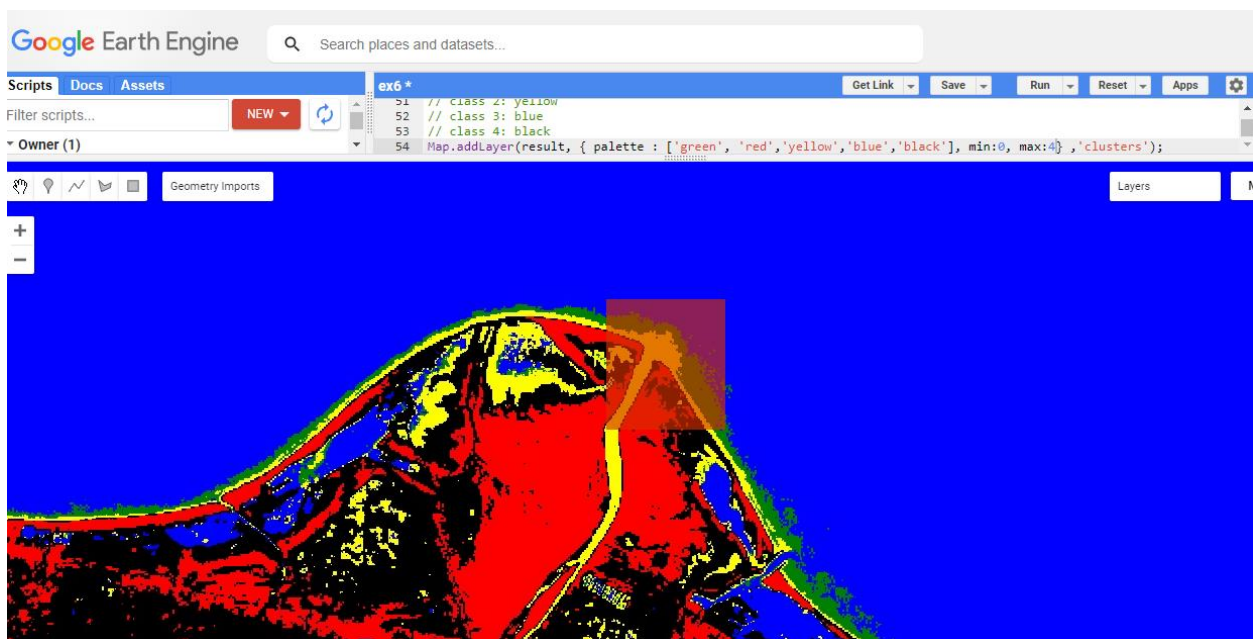
Clustering, an unsupervised machine learning technique, involves grouping similar features together. It examines the input data and identifies natural clusters or groups in the feature space. Now, we will apply the K-means algorithm to classify the input image into four classes that we are interested in identifying within the image.

In line 39 of the code, we are not training the clusterer yet. Instead, we instruct Google Earth Engine (GEE) to prepare the clusterer for the subsequent step, where we will utilize its capability to search for the 5 classes. In line 43, we train the clusterer using the training dataset we created in the first line.

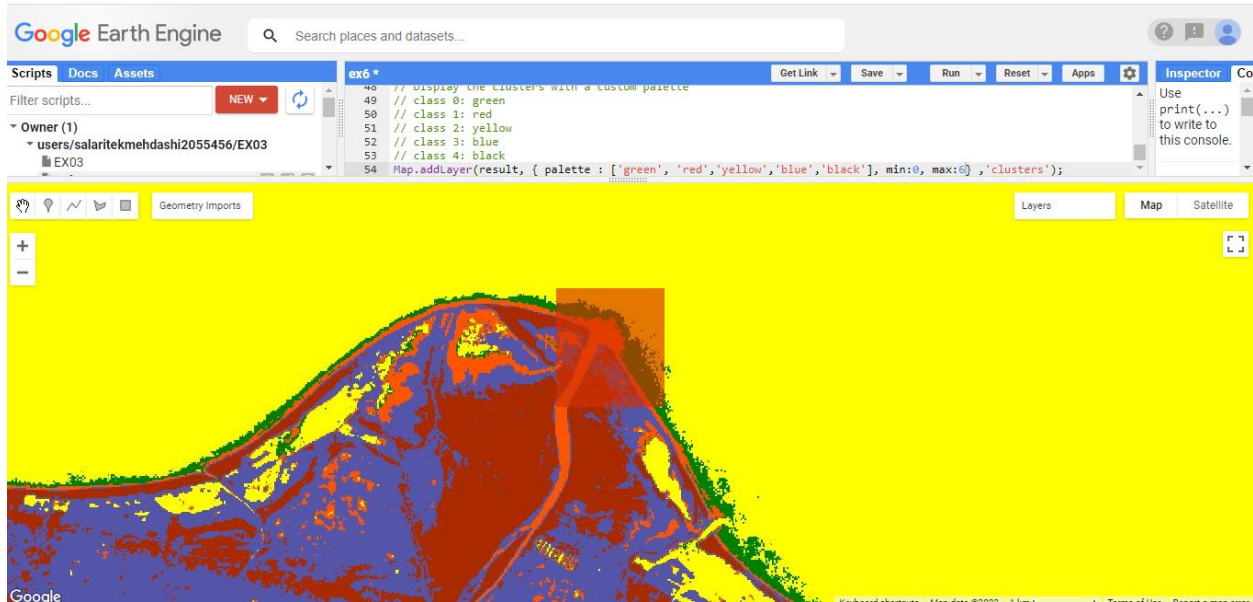
The next step involves using the clusterer to perform inference and predict the class for each pixel in our image. We take the Landsat 7 composite image and apply the clusterer to generate an image with a single band representing the classification. Once we run the code successfully, we can add this resulting image to the map. The unique band in the image will contain five values (0, 1, 2, 3, 4) corresponding to the identified classes.



To add the layer to the map, we have the option to define colors for each class using the palette tool. Without specifying colors, the resulting display will show a spectrum ranging from black to white. However, by utilizing the palette tool, we can assign specific colors to each class based on our desired priority preference.



If we change the number of clusters, we can see changes on the map, Increasing the number of classes leads to a more detailed representation on the map.



## Conclusion:

Utilizing machine learning techniques in Google Earth Engine, particularly through clusterers like K-means, provides powerful capabilities for the analysis of geospatial data. These techniques allow for the clustering of pixels based on their spectral characteristics, enabling the identification of patterns and distinct classes within the dataset and offering valuable insights. When applied to cloud-free Landsat 7 Top of Atmosphere (TOA) composites generated from raw Landsat 7 images, machine learning clustering algorithms enable the classification of pixels within a specific area of interest (AOI) and temporal period. This classification process extracts essential information, enhancing our understanding of the landscape. The resulting clusters, referred to as the "classification\_result," can be effectively visualized using a customized palette. This visualization approach facilitates the interpretation and analysis of the geospatial data, making it easier to identify and comprehend the clusters. In conclusion, the utilization of machine learning and clustering techniques in Google Earth Engine empowers researchers, scientists, and analysts to gain valuable insights and make well-informed decisions across various applications, such as land cover classification, object detection, and change detection.

<https://code.earthengine.google.com/4d2e86dd329bbcf3d4dd79f3391049f5>



